THE JOURNAL OF BIOLOGICAL CHEMISTRY VOL. 286, NO. 1, pp. 661–673, January 7, 2011
Printed in the U.S.A.

Structural and Biological Properties of the *Drosophila* Insulin-like Peptide 5 Show Evolutionary Conservation*[S]

Received for publication, June 18, 2010, and in revised form, October 21, 2010 Published, JBC Papers in Press, October 25, 2010, DOI 10.1074/jbc.M110.156018

Waseem Sajid[‡1], Nikolaj Kulahin[‡], Gerd Schluckebier[§], Ulla Ribel[§], Hope Rosalind Henderson[¶], Marc Tatar[¶], Bo Falck Hansen[§], Angela Manegold Svendsen[‡], Vladislav V. Kiselyov[‡], Per Nørgaard[§], Per-Olof Wahlund[§], Jakob Brandt[§], Ronald A. Kohanski[‖], Asser Sloth Andersen[§], and Pierre De Meyts[‡]

From the [‡]Receptor Systems Biology Laboratory, Insulin and Incretin Biology, Hagedorn Research Institute, 2820 Gentofte, Denmark, the [§]Diabetes Research Unit, Novo Nordisk A/S, 2760 Måløv, Denmark, the [¶]Department of Ecology and Evolutionary Biology, Brown University, Providence, Rhode Island 02912, and [‖]NIA, National Institutes of Health, Bethesda, Maryland 20892

We report the crystal structure of two variants of *Drosophila melanogaster* insulin-like peptide 5 (DILP5) at a resolution of 1.85 Å. DILP5 shares the basic fold of the insulin peptide family (T conformation) but with a disordered B-chain C terminus. DILP5 dimerizes in the crystal and in solution. The dimer interface is not similar to that observed in vertebrates, *i.e.* through an anti-parallel β-sheet involving the B-chain C termini but, in contrast, is formed through an anti-parallel β-sheet involving the B-chain N termini. DILP5 binds to and activates the human insulin receptor and lowers blood glucose in rats. It also lowers trehalose levels in *Drosophila*. Reciprocally, human insulin binds to the *Drosophila* insulin receptor and induces negative cooperativity as in the human receptor. DILP5 also binds to insect insulin-binding proteins. These results show high evolutionary conservation of the insulin receptor binding properties despite divergent insulin dimerization mechanisms.

The ligands and receptors of the insulin peptide family constitute an ancient metazoan signaling system that plays a crucial pleiotropic role in cell growth, metabolism, reproduction, and longevity (1–7).

The mammalian insulin receptor belongs to the family of receptor-tyrosine kinases and is composed of two α subunits and two β subunits linked together by disulfide bonds (for review, see Refs. 4 and 8–10). The existence of a homologue of the mammalian insulin receptor in *Drosophila melanogaster* (DIR)[2] was suggested in 1985 by Petruzzelli *et al.* (11), who identified a glycoprotein of 350–400 kDa that binds bovine insulin specifically with moderate affinity (15 nM). The cDNA sequence of the DIR is remarkably similar to that of the mammalian insulin and IGF-I receptors (with 33% sequence identity) except for substantial N- and C-terminal extensions (12, 13).

In evolution, there is a single receptor from Cnidarians up to and including Amphioxus (*Branchiostoma californiense*), the phylum closest to vertebrates (for review see Refs. 1, 4–6). In vertebrates, gene duplications resulted in three related receptors; that is, the insulin receptor, the type I IGF receptor, and the orphan insulin receptor-related receptor (1, 5).

In humans, members of the insulin peptide family include insulin, the insulin-like growth factors I and II, and seven relaxin-related peptides (for review, see Ref. 14). The same basic fold is shared for all molecules in the superfamily whose structure is known; the B domain contains a single α-helix that lies across the two α-helices of the A domain (15) and two canonical disulfide bridges that connect the A-and B-chains, whereas an intrachain disulfide bridge is present in the A-chain.

The *D. melanogaster* genome contains seven insulin-like genes that are expressed in a highly tissue- and stage-specific patterns, *dilp1–7* (16). *dilp2* is the most related to human insulin with 35% sequence identity, whereas *dilp5* has 27.8% identity (16).

So far, the structures of only two invertebrate insulin-like peptides have been determined by NMR using total peptide synthesis; that is, bombyxin-II (17) and *Caenorhabditis elegans* INS-6 (18). We report here the first crystal structure of invertebrate insulins expressed from cloned cDNAs, namely two variants of DILP5, DB and C4, that differ by the absence or presence of an Asp-Phe-Arg sequence extension at the N terminus of the A-chain. The structures demonstrate a conservation of the classical insulin fold with interesting variations and an unusual dimer structure compared with other known insulins.

In addition, we characterize in detail the properties of human insulin and DILP 5 binding to the human and *Drosophila* insulin receptors as well as to two insect insulin-binding proteins; that is, the insulin-related peptide-binding protein from *Spodoptera frugiperda* (sf-IBP), and the imaginal morphogenesis protein-Late 2 (IMP-L2) from *D. melanogaster*. Moreover, we study the sugar lowering potency of DILP5 *in vivo* in rats and flies. We discuss the implications of our findings in the context of the structural biology and evolution of the insulin/receptor system.

* This work was authored, in whole or in part, by National Institutes of Health staff.

[S] The on-line version of this article (available at http://www.jbc.org) contains supplemental information, Figs. 1–7, and Table 1.

The atomic coordinates and structure factors (codes 2WFV and 2WFU) have been deposited in the Protein Data Bank, Research Collaboratory for Structural Bioinformatics, Rutgers University, New Brunswick, NJ (http://www.rcsb.org/).

[1] To whom correspondence should be addressed. Tel.: 45-44431242; Fax: 45-44438000; E-mail: wsaj@hagedorn.dk.

[2] The abbreviations used are: DIR, *D. melanogaster* insulin-like receptor; DILP5, *D. melanogaster* insulin-like peptide 5; HIR, human insulin receptor; IMP-L2, imaginal morphogenesis protein-Late 2.

EXPERIMENTAL PROCEDURES

Production of Recombinant Proteins—The cDNA encoding dilp5 was obtained by RT-PCR from *D. melanogaster* (OreR) ovaries mRNA. The C4 version of DILP5 consisted of amino acids 24–51 (B-chain, B2–29) and 84–108 (A-chain, A1–25) (Uniprot code Q7KUD5), and the DB version consisted of amino acids 24–51 (B-chain, B2–29) and 87–108 (A-chain, A4–25) (Uniprot code Q7KUD5). The cDNAs were subcloned into the yeast vector pIM45. The pIM45 vector was designed to optimize the insulin expression and is similar to the pAK405 vector (19). *Saccharomyces cerevisiae* strain MT663 was used for expression. Experimental details about fermentation procedure are given in the supplemental information.

The secreted single-chain insulin precursor of the C4 or DB variants was purified from the yeast supernatant by cation exchange (20). The precursor was matured into two-chain insulin by digestion with the lysine-specific protease *Achromobacter lyticus* (Novo Nordisk A/S) (21). The two-chain insulin molecule was purified by reversed phase HPLC (Waters 600 system) on a C18 column using an acetonitrile gradient. The purity of the protein was estimated by analytical LC (Waters Acquity Ultra-Performance Liquid Chromatography system) on a C18 column, and the molecular weight was confirmed by mass spectrometry (Bruker Daltonics Autoflex II TOF/TOF). Finally, gel filtration was performed in 10 mM Hepes, pH 7.4, 20 mM NaCl (for crystallization experiments) or phosphate-buffered saline (PBS) using a PD-10 column (GE Healthcare).

Dynamic Light Scattering—Dynamic light scattering was performed using a DynaPro Titan Temperature Controlled MicroSampler (Wyatt Technology Corp., Santa Barbara, CA). All measurements were performed at 25 °C, and the data were then processed using the DYNAMICS software (Wyatt Technology Corp.).

Crystallization and Structure Determination—Details of proteins crystallization, data collection, and processing and refinement statistics are given in the supplemental information. Briefly, crystallization of the proteins was carried out in hanging-drop vapor-diffusion experiments by mixing 1 μl of protein (9 mg/ml) and 1 μl of reservoir solution (20% PEG 4000). Both variants C4 and DB crystallized in the same space group P43212 with cell parameters $a = b = 40.45$ Å, and $c = 45.24$ Å for DILP5-C4 and $a = b = 39.79$ Å, and $c = 45.32$ Å for DILP5-DB. The structure of DILP5-C4, which contains six cysteines, was solved by means of sulfur single wave length anomalous dipersion phasing using data collected at a wavelength of 1.5418 Å (Cu-Kα) with Sharp/Autosharp (22). The structure of DILP5-DB was determined by molecular replacement with Phaser (23) using the structure of DILP5-C4 as a search model, Both structures were refined at 1.85 Å (see supplemental Table 1 for details). The quality of the electron density map is shown in supplemental Fig. 7. The atomic coordinates and structure factor files corresponding to DILP5-C4 (PDB code 2WFV) and DILP5-DB (PDB code 2WFU) have been deposited in the Protein Data Bank.

Competition assays were done as described earlier (24). IM9 or S2 cells were incubated with [^{125}I] human insulin (20,000 cpm/ml) and increasing concentrations of unlabeled ligand for 1 h for S2 cells and 2.5 h for IM9 cells at 15 °C, pH 7.6. Duplicate aliquots were centrifuged, and bound [^{125}I]human insulin was counted. Two additionally duplicate pooled aliquots were counted as total. Fitting of the data were done according to Wang (25) and Kiselyov *et al.* (26). The details are given in the supplemental information. The insulin analogues X92 (TA8H, HB10D, and B25 Y-amide), X92DOP (TA8H, HB10D, and Des B23-B30), DOP (Des B23-B30), and H2 (TA8H, EB4H, HB10D, and TB27H) were from Novo Nordisk A/S.

Dissociation assays were performed as described (27). IM9 or S2 cells were preincubated with [^{125}I]human insulin for 90 min at 15 °C. The cells were then resuspended in binding buffer at the initial volume. Duplicate aliquots were diluted 40-fold in the absence or presence of 170 nM unlabeled ligand and incubated at 4, 15, and 25 °C. The cells were centrifuged, and the bound activity was counted. Duplicate aliquots of 25 μl of preincubated cell suspension were counted as the time 0. To obtain a dose-response curve for negative cooperativity, duplicate aliquots were diluted 40-fold in the presence of increasing concentrations of unlabeled ligand for 30 min at 15 °C (28).

C4 Binding to sf-IBP and IMPL2—The production of sf-IBP and IMPL2 and the binding assays are described in Sloth *et al.* (29). Briefly, sf-IBP/IMPL2 was incubated for 16 h at 4 °C with ^{125}I-labeled Tyr^{A19} C4 and increasing amounts of unlabeled insulin or C4. Bound counts were recovered by precipitation with 2% γ-globulin and 30% (w/v) polyethylene glycol 8000 and counted in a γ-counter.

Cell Proliferation Assay—DNA synthesis was quantified as [^{3}H]thymidine (Amersham Biosciences) incorporation into DNA according to Bonnesen *et al.* (30) and Gauguin *et al.* (31).

Lipogenesis in Isolated Rat Adipocytes—Glucose incorporation into the lipid phase was determined in primary rat (Sprague-Dawley) adipocytes as described before (32).

Effect of DILP5s on Blood Glucose Level in Rats—The blood glucose lowering effects of the ligands were measured using male Sprague-Dawley rats according to Schäffer *et al.* (32). Briefly, at $t = 0$, human insulin and DB were injected intravenously in the tail, and blood samples were collected at different time points. Each ligand was tested in four rats, and the experiment was repeated three times.

Effect of DILP5s on Trehalose Level in Flies—The experiments were performed as described (33). Briefly, flies at time 0 were sham-injected with PBS, and flies for collection at later times were injected with insulin diluted in PBS to a final concentration of 0.01 mg/ml into the intersegmental integument of the abdomen. Flash-frozen samples for each time point were prepared from five flies pooled together. Trehalose content was determined by estimating the glucose content of each sample before and after digestion with trehalase. Each pooled sample was homogenized in 1 ml of ice-cold buffer (0.01 M KH_2PO_4, 1 mM EDTA, pH 7.4, plus protease inhibitors (CompleteMini, Roche Applied Science). Homogenates

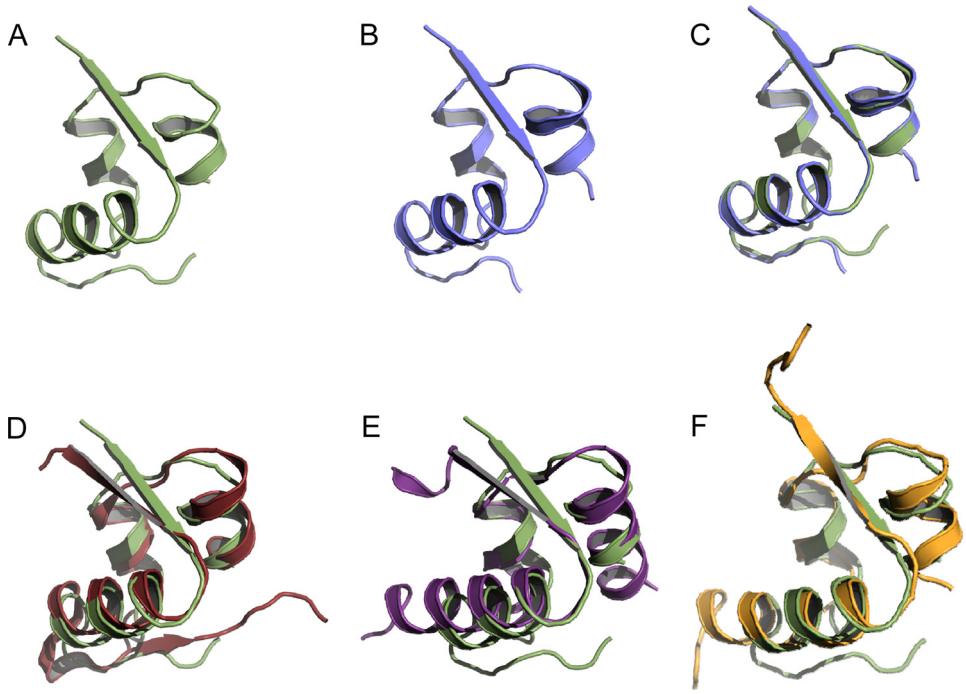

FIGURE 1. **Structural representations of the insulin family peptides.** *A*, shown is DILP5 DB. *B*, shown is DILP5 C4. *C*, shown is superimposition of DB (*green*) and C4 (*blue*). *D*, shown is superimposition of DILP5 (*green*) and human insulin T-form (*red*; PDB code 1MSO). *E*, shown is superimposition of DILP5 (*green*) and human relaxin (*purple*; PDB code 6RLX). *F*, shown is superimposition of DILP5 (*green*) and bombyxin II (*orange*; PDB code 1BOM).

were centrifuged, and five replicates of 2.5 μl from each supernatant were assayed in a 96-well plate for glucose content using Infinity Glucose (Hexokinase) reagent (ThermoElectron). After the initial readout, porcine kidney trehalase (Sigma, T8778) at the concentration of 0.05 units/ml was added to each well. Plates were covered and incubated overnight at 37 °C, and optical density was measured at 340 nm.

RESULTS

Crystal Structure of DILP5—Both DILP variants (C4 and DB) crystallized readily in space group $P4_32_12$ with one molecule in the asymmetric unit and diffracted to a resolution of 1.85 Å.

Because of the high quality of the dataset and to avoid model bias, the structure of DILP5-C4 was determined by sulfur single wave length anomalous dipersion phasing using Autosharp/Sharp (22). Both structures fold basically identically (Fig. 1, *A*–*C*). Residues B25–29 (SMFAK) of C4, B26–29 (MFAK) of DB, and A1–2 (DF) of C4 were not defined by the electron density due to flexibility and consequently were not included in the final model.

DILP5 folds similarly to other proteins of the insulin family such as human insulin, human relaxin, and bombyxin II from *Bombyx mori.* DILP5 and human insulin share 27.8% of sequence identity. When compared with the x-ray structure of human insulin (PDB code 1MSO), the major conformational differences are found in the C-terminal region of the B-chain, which is more flexible and consequently more disordered in DILP5. DILP5 does not fold into a β-turn after the C terminus of the B-chain helix (B20–23 GERG) and consequently is in an extended conformation so that the C terminus is pointing in a different direction when compared with insulin (Fig. 1*D*).

The N terminus of the B-chain of DILP5 exhibits a folding surprisingly comparable with the T-state of human insulin with first residues B1–5 (NSLRA) extended similarly to the N-terminal B1–6 residues of insulin (FVNQHL). Structures of DILP5 and the T-form of insulin display a root mean square deviation of 1.57 Å when superimposing 37 corresponding C-α atoms (the rest of the residues were rejected with the cut-off of 3.67 Å using the default alignment algorithm in PyMOL; Fig. 1*D*).

DILP5 demonstrates lower sequence identity to human relaxin (PDB code 6RLX) (17.2%) compared with human insulin. Structural similarity between DILP5 and human relaxin is described by a root mean square deviation of 1.2 Å based on 26 C-α atoms (the rest of residues were rejected with the cut-off of 1.35 Å; Fig. 1*E*). DILP5 and bombyxin-II (PDB code 1BOM) share 20.8% sequence identity, and the structures are similar with an root mean square deviation of 1.33 Å on 31 C-α atoms (the rest of the residues were rejected with the cut-off of 1.54 Å; Fig. 1*F*). Thus, folding of DILP5 resembles the conformation of the T-form of insulin, relaxin, and bombyxin II.

Analysis of packing contacts in DILP5 crystals indicates that DILP5, similarly to relaxin and insulin, crystallizes as a dimer formed by a crystallographic 2-fold axis. The dimerization mode for DILP5 differs from both human insulin and relaxin. In DILP5, the N termini of the B-chains (residues B1–5 NSLRA) form an anti-parallel β-sheet. The whole dimerization interface is formed by residues Phe^{A16}, B1–5 (NSLRA), Pro^{B8}, Ala^{B9}, Asp^{B12}, and Met^{B13} (Fig. 2*A*). In comparing the DILP5 sequences from the genomes of 12 different *Drosophila* species (34), it appears that this interface is well

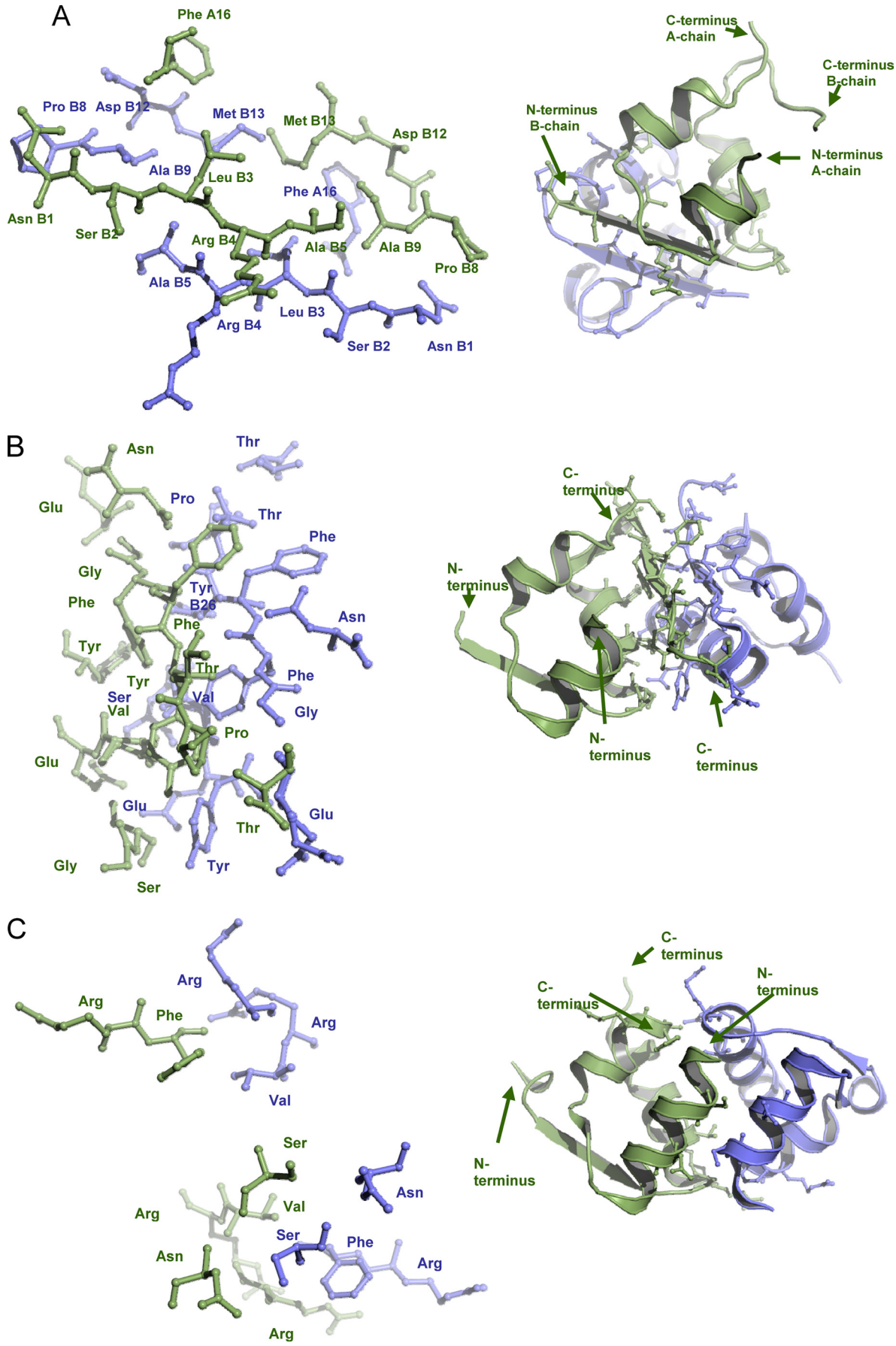
A
Phe A16
Pro B8
Asp B12
Met B13
Met B13
Asp B12
Ala B9
Leu B3
Phe A16
Asn B1
Ser B2
Arg B4
Ala B5
Ala B9
Pro B8
Ala B5
Leu B3
Arg B4
Ser B2
Asn B1
C-terminus A-chain
C-terminus B-chain
N-terminus B-chain
N-terminus A-chain
B
Asn
Thr
Glu
Pro
Thr
Phe
Gly
Tyr B26
Phe
Asn
Phe
Tyr
Thr
Phe
Tyr
Ser
Val
Val
Gly
Pro
Glu
Glu
Glu
Thr
Gly
Tyr
Ser
C-terminus
N-terminus
N-terminus
C-terminus
C
Arg
Arg
Phe
Arg
Val
Ser
Asn
Arg
Val
Ser
Phe
Asn
Arg
Arg
C-terminus
C-terminus
N-terminus
N-terminus

TABLE 1
Comparison of structures of human insulin, human relaxin, and bombyxin II from *B. mori* to the structure of DILP5

	DILP5	Human insulin	Human relaxin	Bombyxin II
PDB code	2WFV	1MSO	6RLX	1BOM
Sequence identity to DILP5 (%)	100	27.8	17.2	20.8
r.m.s.d. (Å) when superimposed on the structure of DILP5	0.0	1.6	1.2	1.3
Number of equivalent C-α atoms used to superimpose molecules	46	73	26	31
Area of buried surface upon dimerization (Å^2)	1129.6	1252.8	1442 Å^2	N/A
Fraction of buried area on total solvent accessible area (%)	17.7	17.2	20.1	N/A

conserved in the DILP5s of a closely related subgroup (*Dmel*, *Dsec*, *Dsim*, *Dyak*, and *Dere*) but not in the other seven species, thus, possibly representing an aggregation mechanism particular to that subgroup. In human insulin several of the equivalent residues are involved in the hexamerization interface and in insulin receptor binding site 2 (4). Analysis of protein packing using the PDBe PISA-server revealed the largest total buried accessible surface area of 1129.6 Å^2 for two molecules of DILP5 (17.65% of total solvent-accessible area), indicating that DILP5 could dimerize in solution (35). The same analysis was performed for dimerization interfaces of human insulin and human relaxin. A buried interface area for two insulin molecules of 1252.8 Å^2 (17.2% of total solvent-accessible area) was calculated. Residues mostly contributing to the dimerization are Asn^{A21}, Gly^{B8}, Ser^{B9}, Val^{B12}, Glu^{B13}, Tyr^{B16}, Glu^{B21}, B23–28 (GFFYTP), and Thr^{B30} (Fig. 2*B*). For relaxin, a buried interface area for two molecules involved in dimerization was calculated to be 1442 Å^2 (20.1% of total solvent-accessible area). Relaxin residues mostly involved in dimerization are Ser^{A4}, Asn^{A8}, Arg^{A22}, Phe^{A23}, Arg^{B13}, Val^{B16}, and Arg^{B17} (Fig. 2*C*). Thus, the relative size of buried interface area for DILP5 is comparable with the corresponding areas for insulin and relaxin, indicating the possibility of DILP5 dimerization in solution (see Table 1 for an overview).

Dynamic light scattering measurements of the protein at the concentration of 0.67 mM revealed that the solution was monodisperse with a hydrodynamic radius of the protein particles of 1.62 nm, consistent with DB and C4 both being dimers in solution. Upon dilution there was a trend toward a smaller hydrodynamic radius, indicating the DILPs were approaching a monomeric state.

Association of ^{125}I Human Insulin to the DIR—The binding of ^{125}I human insulin to DIR is time, temperature, and pH-dependent (supplemental Fig. 1, *A* and *B*). The optimal conditions for binding were found to be 15 °C, pH 6.5, and 60 min of incubation compared with 15 °C, 150 min, and pH 7.6 for HIR. The association was only slightly faster at higher temperatures, and the maximum binding was found after 90 min incubation at 25 °C but was diminished afterward probably due to higher internalization rate compared with the lower temperatures. The equilibrium binding for all temperatures at pH 7.6 was similar, whereas it was different for the association at pH 6.5. The binding was affected by pH with a bell-shaped curve with a pH optimum at about pH 6.5, whereas the optimum for human insulin binding to HIR is pH 8.0 (36).

Dissociation of ^{125}I Human Insulin from the DIR and Negative Cooperativity—The dissociation was also temperature and pH-dependent (supplemental Fig. 2) as it is for the HIR. The dissociation rates increased as the temperature was increased, 25 °C showing the fastest and 4 °C showing the slowest rate. When the pH was lowered from 7.6 to 6.5, the dissociation was markedly decreased at all temperatures examined, which was the opposite effect of what was seen for HIR (28). A clear acceleration of non-first order dissociation was seen at all temperatures and pH values in a 40-fold dilution in the presence of 170 nM unlabeled human insulin, the hallmark of negative cooperativity (27) (see Fig. 3*A*, supplemental Fig. 2). To further investigate this, we performed dose-response curves for accelerated dissociation where the amount of tracer bound after 30 min of dissociation was measured as a function of increasing concentrations of human insulin (Fig. 3*C* and supplemental Fig. 3). Dissociation of ^{125}I human insulin from the HIR by human insulin produced a bell-shaped curve as previously reported (27) and shown in Fig. 3*C*. The same was seen for the DIR, with a rightward shift in the curve reflecting a reduced affinity of human insulin for the DIR Fig. 3*C*. A decrease in the maximal acceleration of dissociation was found when the dose-response curve for negative cooperativity was done at pH 6.5 but the curve was still bell-shaped (supplemental Fig. 3). When the dissociation of prebound ^{125}I human insulin from DIR was carried out in the presence of 5 μM DILP5 DB or C4, a clear acceleration of dissociation was seen to the same extent as when dissociation was carried out in the presence of unlabeled human insulin (Fig. 3*B*). However the dose-response curve for negative cooperativity was sigmoid when the dissociation was carried out in the presence of increasing concentrations of DB or C4 in contrast to the bell-shaped dose-response curve for human insulin (Fig. 3*D*).

Affinities of DILP5s, Human Insulin, and Analogues for the DIR—To compare the binding affinity of DIR and HIR, the affinities of various ligands for DIR were determined in heterologous competition studies using a constant amount of ^{125}I human insulin and increasing concentrations of unlabeled ligands. The average K_d value for each ligand and ±S.D. are shown in Table 2, and the curves are shown in Fig. 4. The

FIGURE 2. **The insulin dimers.** *A*, shown is dimerization of DILP5 with dimerization site consisting of Phe^{A16}, Asn ^{B1}, Ser^{B2}, Lue^{B3}, Arg^{B4}, Ala^{B5}, Pro^{B8}, Ala^{B9}, Asp^{B12}, and Met^{B13}. *B*, shown is dimerization of human insulin with dimerization site consisting of Asn^{A21}, Gly^{B8}, Ser^{B9}, Val^{B12}, Glu^{B13}, Tyr^{B16}, Glu^{B21}, Gly^{B23}, Phe^{B24}, Phe^{B25}, Tyr^{B26}, Thr^{B27}, Pro^{B28}, and Thr^{B30}. *C*, shown is dimerization of human relaxin with the dimerization site consisting of Ser^{A4}, Asn^{A8}, Arg^{A22}, Phe^{A23}, Arg^{B13}, Val^{B16}, and Arg $^{B17.}$ The two monomers are colored in *green* and *blue*. The dimerization site in all three cases consists of residues involved in contacts less than 3.5 Å between monomers (shown as *sticks*).

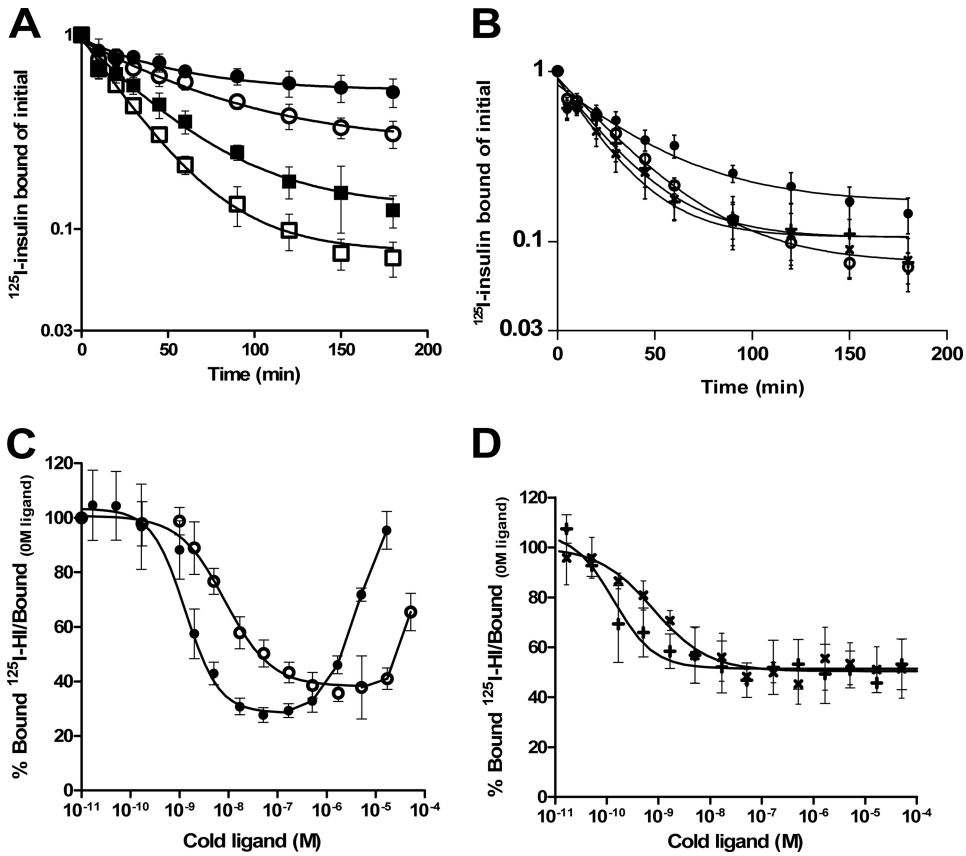

FIGURE 3. **Dissociation assay of ^{125}I human insulin from holo insulin receptor.** *Panel A* shows dissociation of ^{125}I human insulin in dilution alone (*closed symbols*) or in the presence of 170 nM human insulin (*open symbols*) at pH 6.5 (○) and pH 7.6 (□). *Panel B* shows dissociation of ^{125}I human insulin at pH 7.6 in dilution alone (●), in the presence of 170 nM human insulin (○), or in the presence of 5 μM concentrations of either DB (+) or C4 (×). Bound tracer at time *t* as a fraction of bound tracer at time = 0 min was plotted as a function of time. *Panel C* shows a dose-response curve for negative cooperativity for human insulin receptor on IM9 cells (●) and for *Drosophila* insulin receptor on S2 cells (○). Dissociation of prebound ^{125}I human insulin is carried out in the presence of increasing concentrations of cold insulin. *Panel D* shows the dose-response curve for negative cooperativity for *Drosophila* insulin receptor on S2 cells. Dissociation of prebound ^{125}I human insulin is carried out in the presence of increasing concentrations of either cold DB (+) or C4 (×). Curves are illustrated as bound/bound at 0 M cold ligand after 30 min of dissociation. The curves are an average of at least three assays, each made in duplicate.

TABLE 2

Competitive binding for the *Drosophila* insulin receptor of increasing concentrations of human insulin analogues IGFs and the DILP5s (C4 and DB) and a fixed concentration of ^{125}I human insulin

The K_d values are shown as the average ± S.D. K_{d1}, apparent high affinity constant; K_{d2}, low affinity partial site constant. r.m.s.d., root mean square deviation; N/A, not applicable.

Analogue	K_d ± S.D.
	nM
Human insulin	59.6 ± 5
Insulin-like growth factor-I	5913 ± 3188
Insulin-like growth factor -II	30 ± 6.3
Desoctapeptide	468 ± 131
X92 Desoctapeptide	277 ± 47
H2	12.3 ± 3.9
X92 K_{d1}	0.19 ± 0.11
X92 K_{d2}	12.3 ± 5.5
C4 K_{d1}	0.76 ± 0.16
C4 K_{d2}	429 ± 125
DB K_{d1}	0.35 ± 0.09
DB K_{d2}	276 ± 94

DILP5s had the highest affinity (lowest K_d values) for the DIR. The K_d of human insulin for the DIR was 60 nM at pH 7.6, which is higher than the reported 15 nM, pH 7.9, by Petruzzelli *et al.* (37). The K_d for IGF-II was 30 nM, which is lower than 250 nM reported by Petruzzelli *et al.* (11). The above K_d values were obtained by fitting to a single class of sites, but the competition curves for the high affinity ligands were clearly biphasic (Fig. 4, *B* and *D*).

Curve-fitting of the competition experiments was done assuming that there are two independent classes of binding sites (receptor species). Using the harmonic oscillator model of insulin receptor binding (see the supplemental information and supplemental Figs. 5 and 6), one can show that this assumption is not necessary. However, the K_d of the first binding class corresponds to the apparent high affinity binding of the DILP molecule to the cross-linked receptor, and the K_d of the second binding class corresponds to the low affinity partial site of the receptor, whereas the high affinity partial site of the receptor is not "visible" in the competition plot. Thus, this method allows easy quantification of the receptor apparent high affinity binding and also of the binding to the low affinity partial site. In contrast, quantification with the harmonic oscillator model requires measurement of multiple dose-response curves for the accelerated dissociation, which was not attempted in this study. The affinities of the ligands ranked as follows: X92 > DB > C4 ≫ H2 > IGF-II > human insulin ≫ X92DOP > DOP ≫ IGF-I.

Affinities of the Two DILP5s for Human Insulin Receptor—^{125}I-C4 and DB did not show any specific binding to the

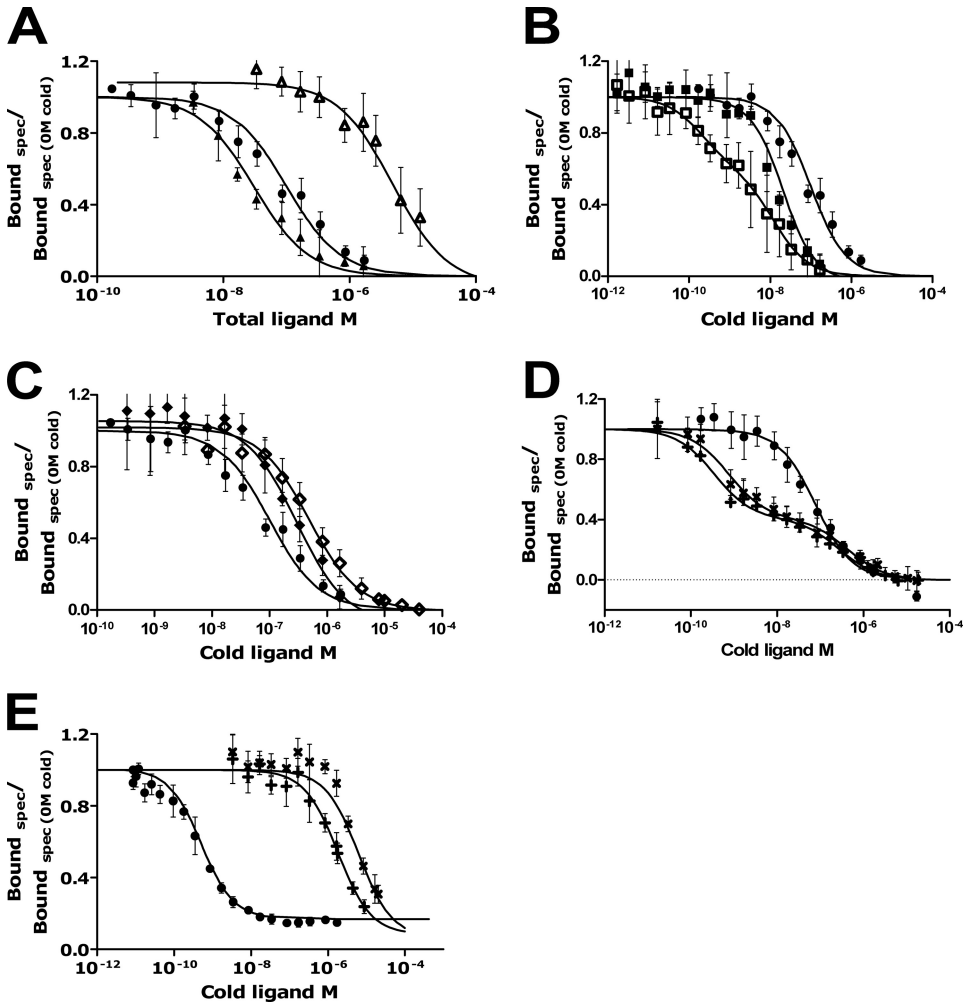

FIGURE 4. **Competition for insulin receptor.** All curves are plotted as specific (*spec*) binding/specific binding at 0 M cold ligand as a function of the concentration of unlabeled ligand at pH 7.6. Competition of ^{125}I human insulin with increasing concentrations of human insulin (●) for DIR on S2 cells is illustrated in all panels. The competition of human insulin at pH 6.5 (○) is compared with pH 7.6 (●). Binding curves show the competing effect of IGF-I (△), IGF-II (▲), X92 (□), H2 (■), DOP (◇), X92DOP (◆), C4 (×), and DB (+). Competition of ^{125}I human insulin with increasing concentrations of human insulin (●), C4 (×), and DB (+) for human insulin receptor on IM9 cells is illustrated in *panel E*. The curves are the averages of at least three assays each made in duplicates.

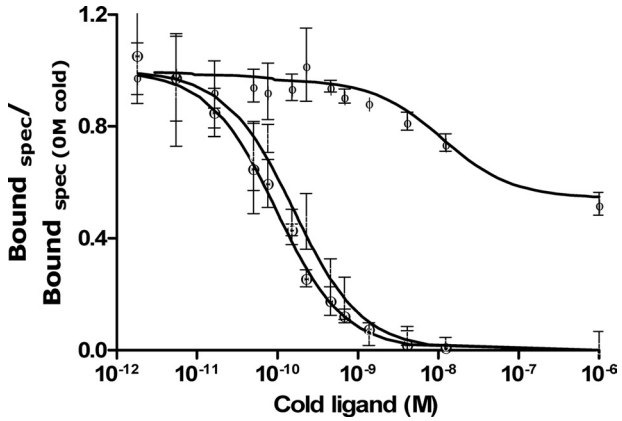

FIGURE 5. **Competition binding to insulin-binding proteins.** Illustrates competition of ^{125}I-C4 with increasing concentrations of C4 for IMPL2 (Θ) and sf-IBP (θ) and with increasing concentrations of human insulin for sf-IBP (Φ). The curves are an average of at least three assays each made in duplicates. *spec*, specific.

human receptor on IM-9 cells. Heterologous competition studies using constant amount of ^{125}I human insulin and increasing concentrations of unlabeled DILP5s, C4 and DB, were carried out to determine the affinities (Fig. 4*E*). The K_d of C4 and DB for the human receptor were much higher than that of human insulin (C4: 5336 nM, DB: 1441 nM and human insulin: 0.36 nM). Those were also surprisingly much higher than the K_d of human insulin for the DIR shown above (60 nM).

Binding of ^{125}I-DILP5 C4 to the Insect-binding Proteins—Even though ^{125}I-DILP5 C4 did not bind to DIR and HIR, it bound well to the insulin-binding proteins from *S. frugiperda* (sf-IBP) and *D. melanogaster* IMPL2 (29). C4 competed with ^{125}I-C4 for the binding proteins (Fig. 5), whereas human insulin displaced C4 only for sf-IBP but with much weaker affinity. Due to a high variation of the assays and a high nonspecific binding (limitations of the PEG assay), we are not able to show average K_d values. The binding of the ^{125}I-Tyr^{A19} DILP5 C4 to the insect-binding proteins was also validated by chemical cross-linking experiments (supplemental Fig. 4), which showed the binding to be specific. ^{125}I-Tyr^{A19} DILP5 DB did not show any specific binding to any of the binding proteins (data not shown).

Mitogenic Potency of DILP5s in L6 Rat Myoblasts Stably Transfected with HIR—The mitogenic potency of the DILP5s were tested against human insulin in a thymidine incorpora-

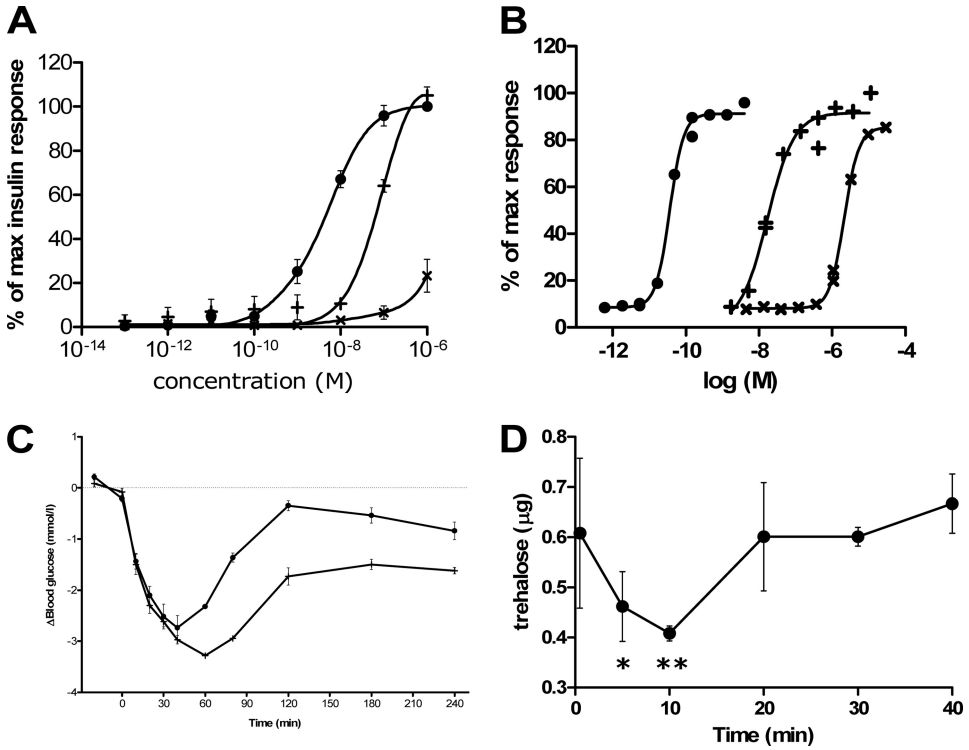

FIGURE 6. **Functional studies of DILP5.** Mitogenic potency is illustrated by [^{3}H]thymidine incorporation of L6 rat muscle myoblasts stably transfected with IR-A (*A*). L6 rat muscle myoblast were treated with increasing concentrations of human insulin (●), C4 (×), and DB (+). The results are illustrated as percent of the insulin response at the highest concentration (10^{-6} M) for each assay. Curves are the average of at least three assays, each made in duplicate, and are fitted using a sigmoidal dose-response curve fit with variable slope. *Panel B* depicts glucose uptake in primary rat adipocytes as a function of increasing concentrations of ligand. [3-^{3}H]Glucose uptake was measured by incubating freshly isolated rat adipocytes with increasing concentrations of human insulin (●), C4 (×), and DB (+). Curves are representative of three assays, each made in duplicate. *Panel C* shows intravenous administration of human insulin and DB in serum-starved Sprague-Dawley rats. The rats were anesthetized before intravenous injection of the ligands. Injection of human insulin 2.5 nmol/kg (●) and DB 500 nmol/kg (+) was performed at time point 0, and 10-μl blood samples were collected from the tail tip 10 time points in addition to a time point before injection. *Panel D* shows the effect of injection of DB on trehalose level in *Drosophila*, Five-day-old female flies were injected with 0.01 mg/ml DB. The mean and S.D. are plotted from samples collected before injection (0 min) and at 5, 10, 20, 30, and 40 min. Trehalose is per 2.5 μl of sample homogenate. $p < 0.05$ (*) and $p < 0.01$ (**) compared with 0 min (one-way analysis of variance with Dunnett's post-test).

tion assay (Fig. 6*A*). The DILP5 DB induced the same maximum response as human insulin (EC_{50}, 3.288 nM ± 0.497), although with a lower potency (EC_{50}, 88.337 nM ± 7.11), whereas the C4 showed a much weaker potency and a much lower maximum at the highest concentrations used.

Effect of DILP5s on Lipogenesis in Primary Rat Adipocytes—Conversion of [^{3}H]glucose into lipids in isolated primary rat adipocytes was used to measure the metabolic potency of the two variants of DILP5 (Fig. 6*B*). Human insulin showed the highest potency with an EC_{50} of 0.0384 nM ± 0.003, the DB had the second highest potency with an EC_{50} of 19.8 nM ± 0.933, and the C4 had the lowest potency with an EC_{50} of 2300 nM ± 110 S.E.

In Vivo Blood Glucose Lowering Effect of DILP5s in Rats—The blood glucose lowering effect of the DILP5s in Sprague-Dawley rats was compared with human insulin (Fig. 6*C*). DB at 500 nmol/kg showed a more profound and more prolonged glucose lowering effect than human insulin at 2.5 nmol/kg, whereas C4 showed no effect at the concentration used, 500 nmol/kg (data not shown).

Trehalose Lowering Effect in Flies—The reducing effect of the DILP5s on the carbohydrate trehalose in adult female *Drosophila* was tested (Fig. 6*D*). Trehalose level was transiently reduced upon injection of 0.2 pmol of DB per fly, whereas the C4 did not show any reduction (data not shown). The reduction of trehalose was initiated immediately and peaked at time 20 min.

DISCUSSION

We report here the crystal structure of two variants of DILP5, DB and C4, that differ by the absence or presence of an Asp-Phe-Arg sequence at the N-terminal end of the A-chain. Although it is not clear which of the two (or both) cleavage sites is used for processing *in vivo*, the fact that DB binds with a higher affinity to the fly and human insulin receptor and has stronger *in vivo* and *in vitro* biological effects suggests that both may have distinct roles that need to be clarified in further studies.

The structure of both DILP5 monomers is very similar to that of mammalian insulins (38) as well as hagfish insulin (39) and the general fold is that of all other members of the insulin-like peptide family including relaxin and bombyxin II (4). The major difference is a more disordered structure of the C terminus of the B-chain in DILP5s, which has major implications regarding the dimerization and receptor binding mechanisms as discussed below.

Both DILP5 variants form dimers in the crystal that were shown by dynamic light scattering to also exist in solution. Strikingly, the DILPs use a very different dimer interface in

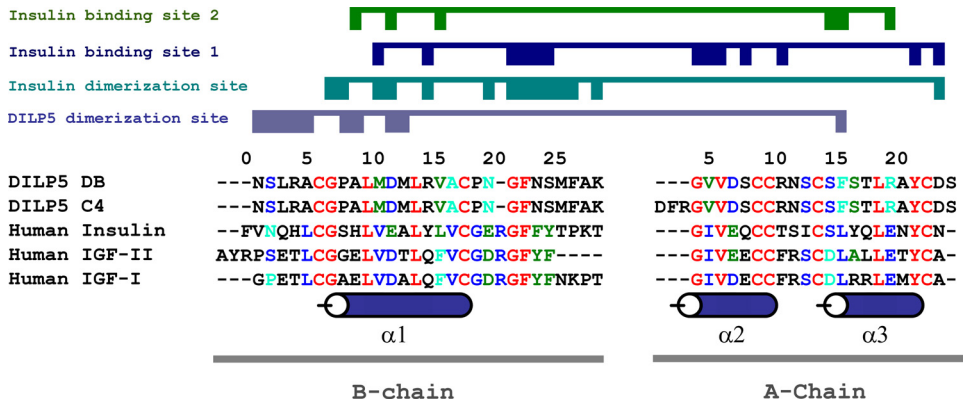

FIGURE 7. **Amino acid sequence alignment.** The conserved amino acids are shown in *red*, whereas the conservative substitutions are shown in *blue*. The similar blocks are shown in *green*, and weakly similar amino acids are in *cyan*. The A- and B-chain for the DILP5 and human insulin share 23 and 43% sequence identity, respectively. The A and B domains of IGF-II share 32 and 43% sequence identity, respectively, with DILP5, whereas the IGF-I share 28 and 48% sequence identity. Numeration and secondary structure elements are shown for DILP5.

the crystal structures (Fig. 7) as compared with the known structures of vertebrate insulin dimers.

It has been demonstrated that insulin residues Asn^{A21}, Val^{B12}, Tyr^{B16}, Gly^{B23}, Phe^{B24}, Phe^{B25}, and Tyr^{B26} from the "classical receptor binding surface" of insulin are part of the dimerization surface (4, 40). In the case of DILP5, the corresponding amino acids are not involved in self-association, possibly suggesting another mechanism of binding between DILP5 and the *Drosophila* insulin receptor (see Fig. 7).

It is remarkable that despite the evolutionary distance between *D. melanogaster* and human insulins, they clearly bind to each other's insulin receptor, albeit with much lower affinity than the cognate ligand. Our demonstration of human insulin binding to the DIR confirms studies of Petruzzelli *et al.* (11, 37) showing binding of bovine insulin to a membrane preparation from frozen fly. The reported affinity was 15 nM at pH 7.9 *versus* our 60 nM at pH 7.6, but it is well established that the solubilized receptor can have a substantially higher affinity than the cell-bound receptor depending on the experimental conditions (41).

Wu and Brown (2) recently concluded that "the binding of insect ILP to an insect insulin receptor has yet to be demonstrated." We have now done so. The DILP5s affinities for the DIR are shown here for the first time and are much higher than that of human insulin, 0.51 nM for DB and 0.93 nM for C4. This is in the range observed for human insulin for the human insulin receptor (0.36 nM in this study).

Insulin analogues had relative affinities for the DIR in the same rank orders of potencies as for the human insulin receptor, showing the typical specificity of the insulin receptor. Interestingly, the affinity of IGF-II was slightly higher than that of human insulin for the DIR. This is consistent with the reported high affinity of the A-isoform of the insulin receptor for IGF-II (42) (DIR has no exon 11, which together with alternative splicing appears only in mammals (5)). This is much higher than the affinity for IGF-II reported by Petruzzelli *et al.* (11), but this is easily explained by progress in the manufacturing of IGFs in the last two decades. We found a very low but measurable affinity for IGF-I (6 μM), whereas Petruzzelli *et al.* (11) found no competition with IGF-I but were not able to test such high concentrations.

The pH dependence of ^{125}I human insulin binding to the DIR was different from that of the human insulin receptor, with an optimum of binding at pH 6.5 instead of pH 7.6. Incidentally, this is close to the pH of insect hemolymph (43). This resulted in higher insulin binding and much slower dissociation rate of ^{125}I human insulin from the DIR. The shift in pH dependence is likely due to a substitution of the equivalent residue in HIR Lys^{460} to Asp in the DIR, as the HIR from a leprechaun patient with a Lys^{460} to Glu substitution shows a similar shift in pH dependence (44).

The affinity of the DILP5 variants for the human insulin receptor (A-isoform) on IM-9 cells was finite but very low, 1.4 μM for C4 and 5.3 μM for DB. However, they were able to completely displace ^{125}I human tracer binding at high concentrations. Moreover, as discussed below, they were able at high concentrations to trigger typical insulin-like effects *in vitro* and *in vivo* in mammalian systems.

It is easy to explain the fact that the DILP5s bind to the human insulin receptor, albeit with low affinity, in the light of the currently accepted model of insulin receptor binding, which proposes that the insulin receptor dimer α-subunits comprise two binding sites, site 1 and site 2, disposed in an antiparallel symmetry (45). The insulin molecule features two binding sites on opposite surfaces, site 1 (4, 10, 46) and a site 2 (10, 31). The two sites of insulin alternatively cross-link the two insulin receptor sites, whereas the receptor oscillates harmonically between the two pairs of sites. This model has been supported by the recent crystal structure of the insulin receptor ectodomain (47) and by mathematical modeling in our laboratory (26).

As shown in Fig. 8, although there are substantial substitutions in these two binding surfaces that explain the low affinity of DILP5s for the human insulin receptor, there is sufficient retention of key contacts in both surfaces to explain the retention of low affinity binding. In particular, the critical residues at A1, A3, (48), and A19 in site 1, which are essential for high affinity insulin binding, are conserved. Moreover, substitution of A8 Thr to Arg has a positive effect on insulin affinity.[3] In site 2, A12 Ser is conserved, and B13 Glu is conservatively substituted to Asp. A13

[3] P. De Meyts, unpublished data.

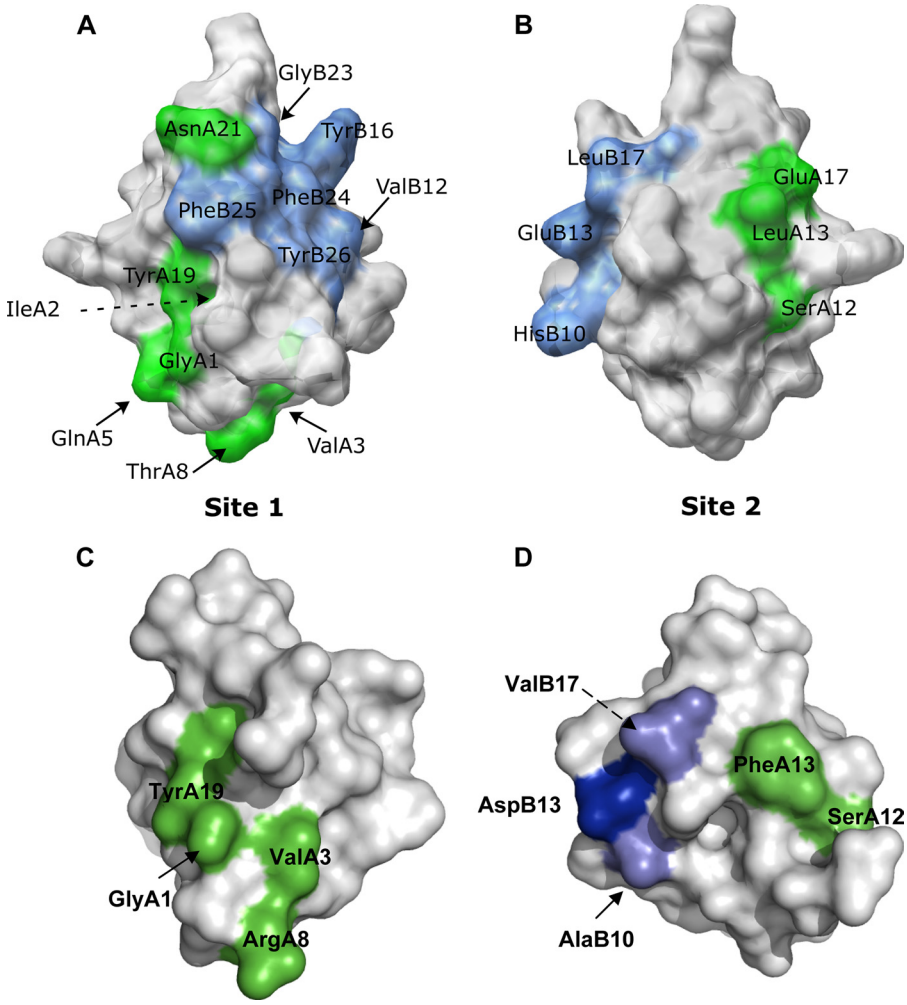

FIGURE 8. **Conservation of insulin and DILP5 binding surfaces involved in binding to the human insulin receptor.** *Panel A* and *B* depict mammalian insulin binding sites 1 and 2 (70). *Panels C* and *D* show the conserved residues that are involved in mammalian insulin binding in a space-fill illustration of DILP5-DB. The residues involved in binding to the receptor are illustrated in *green* (A-chain residues) and *blue* (B-chain residues). The *lighter blue color* represents conservative substitutions. PDB code 9INS (mammalian insulin) and 2WFU (DILP5-DB).

Leu is substituted to Phe, which results in 123% affinity (49), and the substitutions of B10 His to Ala and B17 to Val result in only moderate decreases in affinities to respectively 39 and 42% (50).

The major reason for the low affinity of the DILP5s for the human insulin receptor is clearly the loss of the key contacts at B12, B16, and B23-B26 due to unfavorable substitutions and disordered presentation of the B-chain C terminus. These are also expected to cause a loss of the ability of the DILPs to cause negative cooperativity at the human insulin receptor, as these are essential for negative cooperativity and constitute most of the "cooperative site"(51). However, when we tested the ability of DILP5 to accelerate the dissociation of prebound ^{125}I human insulin, we saw that the DILP5 accelerated the dissociation to the same extent as human insulin, although the concentration used for DILP5 was higher. The dose-response curve for negative cooperativity is sigmoid when the acceleration of prebound human insulin is carried out in the presence of increasing concentrations of DILP-C4 or DILP5-DB rather than bell-shaped when the acceleration is carried out with human insulin. This indicates that the "cooperative site" is conserved enough to accelerate the dissociation but not enough to produce a bell-shaped dose-response curve for negative cooperativity.

The fact that the ^{125}I-labeled DILP5s fails to bind to the DIR and human insulin receptors most likely results from the iodination of the critical Tyr A19, the only conserved Tyr, which is very sensitive to substitutions (mutation to Ala results in 1000-fold loss of affinity). The fact that the labeled C4 retains high affinity for insect binding proteins (see below) shows that the protein was not damaged in the labeling process.

The high affinity binding of DILP5s to the DIR strongly suggests that additional alternative side-chain contacts are used to create high affinity between DILP5s and the DIR, which are not shared by human insulin, which thus binds with about 100 times lower affinity. However, it is noticeable that human insulin still induces negative cooperativity with a bell-shaped curve when accelerated dissociation of prebound HI to DIR is measured, confirming that the structural basis for this mechanism was already embedded in the ancestral receptor (52).

It is, thus, of interest to consider the conservation of the insulin binding elements between the human and *Drosophila*

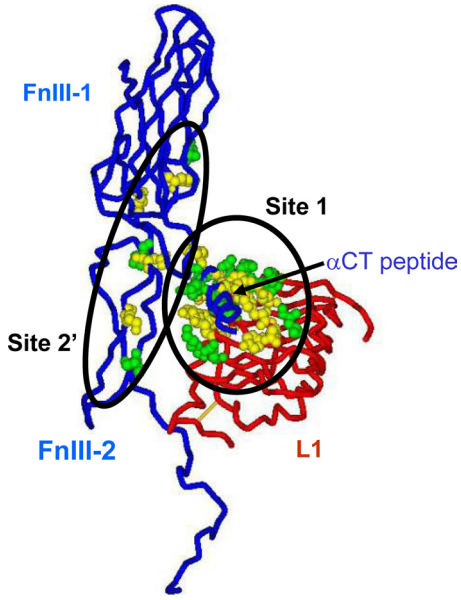

FIGURE 9. **Conservation of receptor residues involved in ligand binding between human and *Drosophila* insulin receptors.** The picture shows the components of one of the two ligand binding sites on the receptor; the L1 domain of one-half human insulin receptor (the backbone in the tube representation is in *red*), and the FnIII-1 and N-terminal portion of the FnIII-2 domain (interrupted at residue 655 where the insert domain, invisible in the structure (53), starts) as well as the αCT peptide of the second half receptor (backbone in tube representation is in *blue*). Insulin is thought to cross-link site 1 and site 2′ (shown here as Corey-Pauling-Koltun balls) as mapped by alanine-scanning mutagenesis of the human insulin receptor; see "Discussion" for details. Site 1 is made of a tandem binding element comprising Leu^{1} residues and the αCT peptide from the opposite receptor half, binding in *trans*, and site 2 is made of residues at the junction of the FnIII-1 and -2 domains. The residues shown in *green* are conserved between the human and *Drosophila* receptors; those shown in *yellow* are not conserved. Four critical residues from the αCT peptide (from alanine scanning data) also conserved between human and *Drosophila* receptors are missing from the structure and, therefore, not shown on the figure: Asn^{711}, Val^{713}, Phe^{714}, and Val^{715}. Sequence comparison was made 1) using multiple alignments of the insulin/IGF-1/insulin receptor-related receptors from multiple species genomes in the RILM data base (University College, London, UK) and 2) by aligning the human and *Drosophila* receptor sequences based on 'blosum62mt2' score matrix using AlignX software (part of Vector NTI software package; Invitrogen). The two alignments gave identical results for the L1 and FnIII domains, but the αCT peptides are not properly aligned in the RILM data base. PDB accession code: 3LOH. The software used for graphics was DSViewerPro (Accelrys, San Diego, CA).

insulin receptors, as mapped by alanine-scanning mutagenesis. Site 1 is comprised of elements from two distinct regions, 1) the central of the three β sheets that make up the L1 domain and 2) the last 16 residues of the α-chain (the so-called α-CT segment, 704–719) from the insert domain in the second fibronectin III domain (53, 54).

Site 2 lies at the junction between the first and second type III fibronectin domains (55). Regarding site 1, the DIR has 10 of 19 of the critical residues conserved in the L1 domain (equivalent to Asp^{12}, Ile^{13}, Arg^{14}, Asn^{15}, Leu^{37}, Phe^{64}, Leu^{87}, Tyr^{91}, Glu^{120}, and Lys^{121} of the HIR) as well as 7 of the 10 residues of the α -CT segment conserved or conservatively substituted (equivalent to Phe^{705}, Glu^{706}, Leu^{709}, Asn^{711}, Val^{713}, Phe^{714}, and Val^{715} of the HIR). Regarding site 2, three of seven residues are conserved or conservatively substituted (equivalent to Leu^{552}, Ile^{603}, and Pro^{621} of the HIR) (Fig. 9).

In line with the conserved but low affinity of the DILP5s for the insulin receptor is the fact that at high concentration DB induces lipogenesis in rat adipocytes and thymidine incorporation in L6 myoblasts expressing the human insulin receptor. This effect is mainly through the insulin receptors as the DILPs were not able to compete with ^{125}I-IGF-I for IGF-I receptors (data not shown). Moreover, DB at high concentrations induced a potent hypoglycemic effect *in vivo* in rats, confirming early observations 30 years ago in mice with crude *Drosophila* extracts (56).

We also show here that DB injected in flies lowered trehalose levels in *Drosophila*, whereas C4 was inactive at the concentrations tested. There is overwhelming evidence from genetic manipulations of a role for invertebrate insulin-like peptides on growth, reproduction, and lifespan (57, 58). Biologists have long suspected that insulin-like peptides might regulate insect carbohydrate metabolism. In early work, bovine insulin injected into hyperglycemic blowflies suppressed trehalose, the primary circulating and storage sugar of insects (59). Recent studies have sought to understand endogenous insulin-like peptides. Bombyxin is an insulin-like peptide produced by neurosecretory cells of the silkworm. In animals, where secretion of endogenous bombyxin was blocked, injection of synthetic bombyxin reduced circulating trehalose, apparently by increasing the conversion of this disaccharide to glucose that is rapidly metabolized by cells (60). In *Drosophila*, ablation of insulin-producing neurons increased whole body levels of trehalose (61, 62). Conversely, trehalose was reduced by transgenic expression of *dilp2* and by injection of bovine insulin (33, 62). Here we demonstrate that recombinant DILP5 has biological activity on metabolism. DILP5 injected into normal adults suppresses whole body trehalose but only transiently as previously reported for injection of bovine insulin (33). Thus, similar to all characterizations of insulin-like peptides in insects, recombinant DILP5 reduces trehalose, the primary sugar of *Drosophila*. Notably, among the seven *Drosophila* insulin-like peptides, mRNA of *dilp5* is most consistently reduced by fasting and dietary restriction (63, 64), suggesting that it may be specialized for metabolic control.

Another important finding is the demonstration here that C4 binds to insulin-binding proteins IMP-L2 from *D. melanogaster* and sf-IBP from the fall armyworm *S. frugiperda* (29, 65, 66). Recent studies have shown that DILPs indeed are associated in a circulating trimeric complex consisting of *Drosophila* homolog of acid-labile subunit and IMP-L2 (65, 66). The antagonizing effect of DILP function and insulin/insulin-like growth factor-like signaling was demonstrated by overexpression of dALS and IMP-L2 *in vivo* in *Drosophila*. The importance of IMP-L2 gene has been demonstrated by genetic studies, which have shown that disruption in the IMP-L2 gene results in embryonic lethality (65, 67, 68). In the starvation resistance study of the larvae, the loss of IMP-L2 leads to a failure to decrease insulin/insulin-like growth factor-like signaling causing high metabolism when the flies need to be shutting down, resulting in starvation sensitive mutants. In a resent study IMP-L2 has been associated with extended longevity in flies upon loss of germ line stem cells where dilp5 is over-

produced (69). The overexpression of IMP-L2 in itself is enough to extend lifespan.[4] A detailed examination of the role of IMP-L2 needs to be made to further elucidate the role of this protein in flies. The specificity of the IMP-L2 has also been shown in that the IGFs were reported to have a slightly higher binding affinity compared with HI (29).

Acknowledgments—We thank Associate professor Leif Søndergaard (University of Copenhagen) for providing the S2 cells, Eva Maria Akke Palmqvist for expression of DILP5 in yeast expression system, and Sofia Håkansson Hederos for purification and maturation of the DILP5.

REFERENCES

1. Adams, T. E., Epa, V. C., Garrett, T. P., and Ward, C. W. (2000) *Cell. Mol. Life Sci.* **57,** 1050–1093
2. Wu, Q., and Brown, M. R. (2006) *Annu. Rev. Entomol.* **51,** 1–24
3. Taguchi, A., and White, M. F. (2008) *Annu. Rev. Physiol* **70,** 191–212
4. De Meyts, P. (2004) *BioEssays* **26,** 1351–1362
5. Hernández-Sánchez, C., Mansilla, A., de Pablo, F., and Zardoya, R. (2008) *Mol. Biol. Evol.* **25,** 1043–1053
6. Rentería, M. E., Gandhi, N. S., Vinuesa, P., Helmerhorst, E., and Mancera, R. L. (2008) *PLoS ONE* **3,** e3667
7. Tatar, M., Bartke, A., and Antebi, A. (2003) *Science* **299,** 1346–1351
8. De Meyts, P., and Whittaker, J. (2002) *Nat. Rev. Drug Discov.* **1,** 769–783
9. Lawrence, M. C., McKern, N. M., and Ward, C. W. (2007) *Curr. Opin. Struct. Biol.* **17,** 699–705
10. De Meyts, P. (2008) *Trends Biochem. Sci.* **33,** 376–384
11. Petruzzelli, L., Herrera, R., Garcia, R., and Rosen, O. M. (1985) *Cancer Cells*, pp. 115–122, Cold Spring Harbor Laboratory, Cold Spring Harbor, NY
12. Fernandez, R., Tabarini, D., Azpiazu, N., Frasch, M., and Schlessinger, J. (1995) *EMBO J.* **14,** 3373–3384
13. Ruan, Y., Chen, C., Cao, Y., and Garofalo, R. S. (1995) *J. Biol. Chem.* **270,** 4236–4243
14. Wilkinson, T. N., and Bathgate, R. A. (2007) *Adv. Exp. Med. Biol.* **612,** 1–13
15. Murray-Rust, J., McLeod, A. N., Blundell, T. L., and Wood, S. P. (1992) *BioEssays* **14,** 325–331
16. Brogiolo, W., Stocker, H., Ikeya, T., Rintelen, F., Fernandez, R., and Hafen, E. (2001) *Curr. Biol.* **11,** 213–221
17. Nagata, K., Hatanaka, H., Kohda, D., Kataoka, H., Nagasawa, H., Isogai, A., Ishizaki, H., Suzuki, A., and Inagaki, F. (1995) *J. Mol. Biol.* **253,** 749–758
18. Hua, Q. X., Nakagawa, S. H., Wilken, J., Ramos, R. R., Jia, W., Bass, J., and Weiss, M. A. (2003) *Genes Dev.* **17,** 826–831
19. Kjeldsen, T., Brandt, J., Andersen, A. S., Egel-Mitani, M., Hach, M., Pettersson, A. F., and Vad, K. (1996) *Gene* **170,** 107–112
20. Kjeldsen, T., Hach, M., Balschmidt, P., Havelund, S., Pettersson, A. F., and Markussen, J. (1998) *Protein Expr. Purif.* **14,** 309–316
21. Kristensen, C., Kjeldsen, T., Wiberg, F. C., Schäffer, L., Hach, M., Havelund, S., Bass, J., Steiner, D. F., and Andersen, A. S. (1997) *J. Biol. Chem.* **272,** 12978–12983
22. De La Fortelle, E., and Bricogne, G. (1997) *Methods Enzymol.* **276,** 472–494
23. Storoni, L. C., McCoy, A. J., and Read, R. J. (2004) *Acta Crystallogr. D Biol. Crystallogr.* **60,** 432–438
24. Sajid, W., Holst, P. A., Kiselyov, V. V., Andersen, A. S., Conlon, J. M., Kristensen, C., Kjeldsen, T., Whittaker, J., Chan, S. J., and De Meyts, P. (2009) *Biochemistry* **48,** 11283–11295
25. Wang, Z. X. (1995) *FEBS Lett.* **360,** 111–114
26. Kiselyov, V. V., Versteyhe, S., Gauguin, L., and De Meyts, P. (2009) *Mol. Syst. Biol.* **5,** 243
27. de Meyts, P., Roth, J., Neville, D. M., Jr., Gavin, J. R., 3rd, and Lesniak, M. A. (1973) *Biochem. Biophys. Res. Commun.* **55,** 154–161
28. DeMeyts, P., Bainco, A. R., and Roth, J. (1976) *J. Biol. Chem.* **251,** 1877–1888
29. Sloth, Andersen, A., Hertz, Hansen, P., Schaffer, L., and Kristensen, C. (2000) *J. Biol. Chem.* **275,** 16948–16953
30. Bonnesen, C., Nelander, G. M., Hansen, B. F., Jensen, P., Krabbe, J. S., Jensen, M. B., Hegelund, A. C., Svendsen, J. E., and Oleksiewicz, M. B. (2010) *Cell Biol. Toxicol.* **26,** 293–307
31. Gauguin, L., Klaproth, B., Sajid, W., Andersen, A. S., McNeil, K. A., Forbes, B. E., and De Meyts, P. (2008) *J. Biol. Chem.* **283,** 2604–2613
32. Schäffer, L., Brissette, R. E., Spetzler, J. C., Pillutla, R. C., Østergaard, S., Lennick, M., Brandt, J., Fletcher, P. W., Danielsen, G. M., Hsiao, K. C., Andersen, A. S., Dedova, O., Ribel, U., Hoeg-Jensen, T., Hansen, P. H., Blume, A. J., Markussen, J., and Goldstein, N. I. (2003) *Proc. Natl. Acad. Sci. U.S.A.* **100,** 4435–4439
33. Belgacem, Y. H., and Martin, J. R. (2006) *J. Neurobiol.* **66,** 19–32
34. Groenke, S., Clarke, D. F., Broughton, S., Andrews, T. D., and Partridge, L. (2010) *PLoS Genet.* **6,** e1000857
35. Krissinel, E., and Henrick, K. (2007) *J. Mol. Biol.* **372,** 774–797
36. De Meyts, P. (1976) in *Methods in Receptor Research* (Blecher, M., ed.) pp. 301–383, Marcel Dekker, Inc., New York
37. Petruzzelli, L., Herrera, R., Garcia-Arenas, R., and Rosen, O. M. (1985) *J. Biol. Chem.* **260,** 16072–16075
38. Baker, E. N., Blundell, T. L., Cutfield, J. F., Cutfield, S. M., Dodson, E. J., Dodson, G. G., Hodgkin, D. M., Hubbard, R. E., Isaacs, N. W., and Reynolds, C. D. (1988) *Philos. Trans. R. Soc. Lond. B. Biol. Sci.* **319,** 369–456
39. Cutfield, J. F., Cutfield, S. M., Dodson, E. J., Dodson, G. G., Emdin, S. F., and Reynolds, C. D. (1979) *J. Mol. Biol.* **132,** 85–100
40. Blundell, T., Dodson, G., Hodgkin, D., and Mercola, D. (1972) *Adv. Protein Chem.* **26,** 279–402
41. Schäffer, L. (1994) *Eur. J. Biochem.* **221,** 1127–1132
42. Frasca, F., Pandini, G., Scalia, P., Sciacca, L., Mineo, R., Costantino, A., Goldfine, I. D., Belfiore, A., and Vigneri, R. (1999) *Mol. Cell. Biol.* **19,** 3278–3288
43. Glaser, R. W. (1925) *J. Gen. Physiol.* **7,** 599–602
44. Kadowaki, H., Kadowaki, T., Cama, A., Marcus-Samuels, B., Rovira, A., Bevins, C. L., and Taylor, S. I. (1990) *J. Biol. Chem.* **265,** 21285–21296
45. De Meyts, P. (1994) *Diabetologia* **37,** Suppl 2, S135–S148
46. Pullen, R. A., Lindsay, D. G., Wood, S. P., Tickle, I. J., Blundell, T. L., Wollmer, A., Krail, G., Brandenburg, D., Zahn, H., Gliemann, J., and Gammeltoft, S. (1976) *Nature* **259,** 369–373
47. McKern, N. M., Lawrence, M. C., Streltsov, V. A., Lou, M. Z., Adams, T. E., Lovrecz, G. O., Elleman, T. C., Richards, K. M., Bentley, J. D., Pilling, P. A., Hoyne, P. A., Cartledge, K. A., Pham, T. M., Lewis, J. L., Sankovich, S. E., Stoichevska, V., Da Silva, E., Robinson, C. P., Frenkel, M. J., Sparrow, L. G., Fernley, R. T., Epa, V. C., and Ward, C. W. (2006) *Nature* **443,** 218–221
48. Huang, K., Chan, S. J., Hua, Q. X., Chu, Y. C., Wang, R. Y., Klaproth, B., Jia, W., Whittaker, J., De Meyts, P., Nakagawa, S. H., Steiner, D. F., Katsoyannis, P. G., and Weiss, M. A. (2007) *J. Biol. Chem.* **282,** 35337–35349
49. Glendorf, T. (1995) *Structure-Function Analysis of the Insulin Molecule by Site-directed Mutagenesis*. M.Sc. thesis, Danish Technical University, Lyngby, Denmark
50. Glendorf, T., Sørensen, A. R., Nishimura, E., Pettersson, I., and Kjeldsen, T. (2008) *Biochemistry* **47,** 4743–4751
51. De Meyts, P., Van Obberghen, E., Roth, J., Wollmer, A., and Brandenburg, D. (1978) *Nature* **273,** 504–509
52. Muggeo, M., Van Obberghen, E., Kahn, C. R., Roth, J., Ginsberg, B. H., De Meyts, B. H., Emdin, S. O., and Falkmer, S. (1979) *Diabetes* **28,** 175–181
53. Smith, B. J., Huang, K., Kong, G., Chan, S. J., Nakagawa, S., Menting, J. G., Hu, S. Q., Whittaker, J., Steiner, D. F., Katsoyannis, P. G., Ward, C. W., Weiss, M. A., and Lawrence, M. C. (2010) *Proc. Natl. Acad. Sci. U.S.A.* **107,** 6771–6776

[4] M. Tatar, unpublished data.

54. Whittaker, J., Sørensen, H., Gadsbøll, V. L., and Hinrichsen, J. (2002) *J. Biol. Chem.* **277,** 47380–47384
55. Whittaker, L., Hao, C., Fu, W., and Whittaker, J. (2008) *Biochemistry* **47,** 12900–12909
56. Meneses, P., and De Los Angeles, Ortíz, M. (1975) *Comp Biochem. Physiol A Comp. Physiol.* **51,** 483–485
57. Chan, S. J., and Steiner, D. F. (2000) *Am. Zool.* **40,** 213–222
58. Claeys, I., Simonet, G., Poels, J., Van Loy, T., Vercammen, L., De Loof, A., and Vanden Broeck, J. (2002) *Peptides* **23,** 807–816
59. Normann, T. C. (1975) *Nature* **254,** 259–261
60. Satake, S., Masumura, M., Ishizaki, H., Nagata, K., Kataoka, H., Suzuki, A., and Mizoguchi, A. (1997) *Comp. Biochem. Physiol. B* **118,** 349–357
61. Broughton, S. J., Piper, M. D., Ikeya, T., Bass, T. M., Jacobson, J., Driege, Y., Martinez, P., Hafen, E., Withers, D. J., Leevers, S. J., and Partridge, L. (2005) *Proc. Natl. Acad. Sci. U.S.A.* **102,** 3105–3110
62. Rulifson, E. J., Kim, S. K., and Nusse, R. (2002) *Science* **296,** 1118–1120
63. Ikeya, T., Galic, M., Belawat, P., Nairz, K., and Hafen, E. (2002) *Curr. Biol.* **12,** 1293–1300
64. Min, K. J., Yamamoto, R., Buch, S., Pankratz, M., and Tatar, M. (2008) *Aging Cell* **7,** 199–206
65. Arquier, N., Géminard, C., Bourouis, M., Jarretou, G., Honegger, B., Paix, A., and Léopold, P. (2008) *Cell Metab.* **7,** 333–338
66. Honegger, B., Galic, M., Köhler, K., Wittwer, F., Brogiolo, W., Hafen, E., and Stocker, H. (2008) *J. BIOL.* **7,** 10
67. Garbe, J. C., Yang, E., and Fristrom, J. W. (1993) *Development* **119,** 1237–1250
68. Osterbur, D. L., Fristrom, D. K., Natzle, J. E., Tojo, S. J., and Fristrom, J. W. (1988) *Dev. Biol.* **129,** 439–448
69. Flatt, T., Min, K. J., D'Alterio, C., Villa-Cuesta, E., Cumbers, J., Lehmann, R., Jones, D. L., and Tatar, M. (2008) *Proc. Natl. Acad. Sci. U.S.A.* **105,** 6368–6373
70. Gauguin, L. (2008) *Structural Basis for the Specific Interaction of Insulin and Insulin-like Growth Factors with Their Receptors.* Ph.D. thesis, University of Copenhagen